Economic Analysis and Optimal Sizing of Battery Storage for Residential Consumers with Solar

Mohammadreza Bakhtiari, Ce Xu, and Yue Zhao
Department of Electrical and Computer Engineering
Stony Brook University
Stony Brook, NY 11794, USA
mohammadreza.bakhtiari@stonybrook.edu, ce.xu@stonybrook.edu, yue.zhao.2@stonybrook.edu

***Abstract*—The economic viability of battery energy storage systems (BESS) for residential consumers with rooftop solar is studied. Hourly BESS charging/discharging decisions are optimized in a stochastic model predictive control (MPC) framework: as time progresses, a) hourly decisions are continuously made; b) forecasts of future solar generation are continuously updated, and c) based on the updated forecasts, scenarios of solar generation in the prediction horizon are repeatedly generated and used as input to the stochastic MPC. Based on the entire trajectory of the optimized BESS charging/discharging decisions, realistic BESS degradation models are employed to accurately evaluate the degradation impact of these decisions. Based on both the entire revenue/payments stream and the degradation process until the end-of-life of a BESS, Internal Rate of Return (IRR) is employed as a universal metric to evaluate the return on investment of the BESS, which fairly compares BESS with different a) specifications and b) lifetimes resulting from its decision history. Based on simulations of optimized BESS operations with real-world data, an accurate and comprehensive economic analysis of a wide variety of BESS specifications is conducted. Optimal BESS sizing that achieves the highest IRR is identified.**

***Index Terms*—Battery, energy storage, degradation, solar energy, economics, return on investment, simulation, stochastic model predictive control**

I. Introduction

There have been a rapidly increasing number of rooftop solar energy systems in power distribution systems around the world [1]. As the cost of battery energy storage system (BESS) continues to decrease, an important question arises: Does it make economic sense to pair rooftop solar with a BESS? Notably, the economic viability for BESS with solar energy heavily depends on the pricing mechanisms for electricity from the grid, for which a wide variety exist (see, e.g., [2]). With Time-of-Use (TOU) prices, for example, excess solar energy during off-peak hours could potentially be stored in BESS for peak-hour usage later, thereby reducing the electricity drawn from the grid during peak hours. While debates on BESS's economic viability in the presence of solar energy have existed for at least a decade since the introduction of Tesla Powerwall, there is still a lack of clarity in answering this question. To provide an accurate answer, realistic and comprehensive simulations of battery operations with solar energy and loads are essential, for which a key factor is to precisely characterize the degradation of BESS in the simulations.

This work is supported by ONR under Award N00014-23-1-2124. The first two authors contributed equally to this work.

Energy storage control in the presence of renewable energies has attracted significant research attention. Given the uncertainties of renewables, a popular approach is stochastic model predictive control [3]–[5], and a variety of renewable energy scenario generation methods have been proposed [6]. However, existing frameworks often do not adequately capture BESS degradation effects in an accurate fashion, especially due to the complex nature of the BESS degradation mechanisms. As such, existing economic analysis of energy storage systems has mainly focused on operational revenue optimization with limited consideration of long-term degradation costs and their impact on economic viability [7]. Comprehensive frameworks that integrate both short-term control decision optimization and long-term economic viability analysis are absent.

In this paper, we study the return on investment and hence the economic viability of BESS for a residential consumer with rooftop solar. Notably, BESS charging/discharging is the only control decision to make: based on such decisions, solar generation and loads, the electricity bought from or sold to the grid can then be determined from the power balance. Importantly, we consider the charging/discharging decisions of BESS to be continuously optimized and executed every hour. In particular, solar energy forecast in the near future, which are continuously updated, are used as part of the input to the optimization program. As such, a stochastic MPC framework is developed for solving BESS changing/discharging decisions: at every hour, a) scenarios of solar generation in a look-ahead window (e.g., 24 hours) are generated based on the solar energy forecast and a stochastic model of forecast errors in this window, b) loads in this look-ahead window are assumed to be known, as near-term load forecast is typically much more accurate than solar energy forecast, and c) prices for buying/selling electricity from/to the grid in all hours are assumed to be known, which is a typical situation for residential energy consumers. A linear cost function is employed in the optimization program to represent the long-term impact of charging/discharging decisions on BESS degradation.

After the BESS charging/discharging decisions are *solved* and implemented, to precisely *evaluate* their impact on the BESS degradation, we employ an *accurate degradation model* of BESS which captures both the cycle degradation and calendar degradation from the entire charging/discharging decision history. Finally, to evaluate the overall life-time return on

investment of BESS, we establish a comprehensive simulation environment based on a) real-world data of loads, prices, and solar generation traces, and b) realistically simulated and continuously updated solar energy forecast based on real-world forecast error statistics. We then simulate the *entire lifetime* of BESS with the optimized hourly charging/discharging decisions. Among all the relevant metrics we observe for BESS's performance, we highlight the *internal rate of return* (IRR) [8] as the key indicator of return on investment and hence economic viability. Through the optimization-and-simulation-based evaluation, an accurate economic analysis of BESS is conducted for a wide range of BESS sizing choices.

II. System Model

We consider a residential home with solar energy and BESS. The system model consists of four components: solar generation, electrical load, BESS, and grid interactions through buying or selling electricity.

A. Solar Generation and Electric Load

Let S_t represent the solar power generation at time t. The solar energy system has a maximum generation of S_{max} according to its rated capacity. We thus have

$$0 \leq S_t \leq S_{max}. \tag{1}$$

Notably, the uncertainty in future solar generation, manifested in errors in its forecast, presents the primary challenge for optimal system operation, as solar generation cannot be directly controlled but depends on weather conditions.

The electrical load of the consumer at time t is denoted by L_t. In this study, we assume accurate knowledge of the future loads in the look-ahead window (e.g., 24 hours) in the MPC.

B. Battery Energy Storage System

The BESS is characterized by several key parameters that define its operational capabilities and constraints.

1) BESS Specifications: The BESS model is as follows:

- Energy capacity E_{cap} (kWh): The maximum amount of energy that could be stored.
- Power capacity P_{cap} (kW): Maximum charging and discharging rate.
- Charging efficiency η_c: Energy conversion efficiency during charging.
- Discharging efficiency η_d: Energy conversion efficiency during discharging.
- State of charge bounds: minimum SOC_{min} and maximum SOC_{max}.

The *duration* of the BESS can be calculated as $\frac{E_{cap}}{P_{cap}}$.

2) State of Charge Dynamics: The battery state of charge changes according to the charging and discharging decisions. We denote the BESS charging/discharging decision variable at time t by P_t^{batt}: When $P_t^{batt} < 0$, the battery is charging with power $|P_t^{batt}|$; when $P_t^{batt} > 0$, the battery is discharging with power P_t^{batt}. We also have,

$$P_{cap}^{ch} \leq P_t^{batt} \leq P_{cap}^{dis}, \tag{2}$$

where P_{cap}^{ch} and P_{cap}^{dis} represent the maximum charging and discharging power limits, respectively.

We denote the state of charge at time t by SOC_t. The SOC dynamics are governed by:

$$SOC_{t+\Delta t} = SOC_t + \eta_c \cdot \max(-P_t^{batt}, 0) \cdot \Delta t - \frac{\max(P_t^{batt}, 0)}{\eta_d} \cdot \Delta t, \tag{3}$$

where Δt is the duration of the time step. The state of charge satisfies the operational constraints:

$$SOC_{min} \leq SOC_t \leq SOC_{max}, \quad \forall t. \tag{4}$$

3) Battery Degradation Model: Battery degradation occurs through two primary mechanisms: cycle-based degradation from charging and discharging operations, and calendar-based degradation from aging over time [9].

Similar to the material fatigue under stress cycles, the battery degradation exhibits cycle-based characteristics where cycle depth affects degradation in a nonlinear way. Deeper cycles usually cause a higher battery degradation rate. This can be modeled in a polynomial relationship [10]:

$$\Delta D_{cycle} = \sum_k \frac{1}{N_k} \cdot \left(\frac{DoD_k}{100} \right)^{2.03}, \tag{5}$$

where ΔD_{cycle} is a battery degradation indicator, normalized between 0 (indicating new battery at an initial capacity of 100%) and 1 (indicating battery at 0% capacity). DoD_k is the depth of discharge at a discretized level k, and N_k is the cycle count at that depth. These cycles and counts can be extracted by the *Rainflow cycle-counting algorithm* [11] based on the *entire* SOC trajectory over time. Notably, this algorithm does not lend itself to closed-form expressions. On the other hand, Calendar-based degradation accumulates as a function of time:

$$\Delta D_{calendar} = \alpha_{calendar} \cdot \Delta t, \tag{6}$$

where $\alpha_{calendar}$ is the calendar degradation rate. A total battery degradation indicator is then defined as:

$$\Delta D_{total} = \Delta D_{cycle} + \Delta D_{calendar}. \tag{7}$$

Furthermore, in multi-year operations, the battery experiences higher degradation in the early stages of its life than later. This phenomenon is the result of the formation of the Solid Electrolyte Interphase (SEI) film [9]. Empirically, it is observed that actual BESS's loss of life has a non-linear relationship with the above defined ΔD_{total}, modeled by

$$C_{remaining} = \alpha_{sei} e^{-\beta_{sei} \Delta D_{total}} + (1 - \alpha_{sei}) e^{-\Delta D_{total}}, \tag{8}$$

where $C_{remaining}$ is the remaining battery life in percentage of its initial capacity. α_{sei} and β_{sei} are parameters related to solid electrolyte interphase formation, and can be obtained by fitting empirical test data. The battery is considered to have reached the end of life when the remaining capacity $C_{remaining}$ drops below a certain threshold, e.g., 70%.

4) Battery Cost: We denote the capital cost of BESS by c_{batt}. It consists of the energy component and the power inverter component:

$$c_{batt} = c_E + c_P = E_{cap} \cdot \pi_E + P_{cap} \cdot \pi_P, \tag{9}$$

where π_E and π_P are the costs of the energy storage component per kWh and the power inverter component per kW.

C. Grid Interaction and Pricing Mechanism

The system interacts with the electrical grid through buying and selling electricity. Let P_t^{buy} represent the power purchased from the grid and P_t^{sell} the power sold to the grid at time t. We define the following notations:

- Buying price π_t^{buy}: Cost of purchasing a unit of electricity from the grid at time t.
- Selling price π_t^{sell}: Revenue from selling a unit of electricity to the grid at time t.

π_t^{buy} and π_t^{sell} can vary over hours and days. As such, this model is a general one that encompasses a variety of real-world pricing mechanisms such as flat rates and time-of-use (TOU) pricing. In summary, Figure 1 depicts the overall structure of the system model and how energy flows between the solar energy system, load, BESS, and grid.

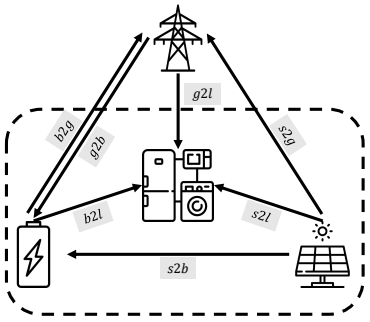

Fig. 1. Interactions between solar energy, load, BESS, and grid.

III. Methodology

In this section, we present our methodology for both a) optimizing BESS charging/discharging under uncertainties, and b) evaluating BESS's return on investment based on such optimized control.

A. Stochastic Model Predictive Control

We employ a two-stage stochastic MPC approach with a 24-hour prediction horizon that rolls forward hourly. At each hour, the controller solves an optimization problem over multiple solar generation scenarios of the next 24 hours, and implements only the first hour's decision. Importantly, at each hour, new solar generation scenarios are generated based on the *latest* forecast information available at that hour. As time progresses, the optimization problem is solved repeatedly. The details of solar scenario generation in our simulations are presented later in Section III-C.

Specifically, in the stochastic MPC program, the first stage decisions are for the current hour, and are denoted by P_0^{batt}, P_0^{buy}, and P_0^{sell}. The second stage decisions are for scenarios of future hours, and are denoted by $P_{t,i}^{batt}$, $P_{t,i}^{buy}$, and $P_{t,i}^{sell}$, where i denotes the scenario index.

The objective is to minimize the expected operational costs:

$$\min \left[Cost_0 + \frac{1}{N_{scen}} \sum_i \sum_{t=1}^{T-1} Cost_{t,i} \right], \tag{10}$$

where the cost includes energy cost via grid interactions and battery degradation cost (in which we omit the scenario index for brevity):

$$Cost_t = \pi_t^{buy} P_t^{buy} - \pi_t^{sell} P_t^{sell} + \alpha_{deg} |P_t^{batt}|. \tag{11}$$

Notably, the actual long-term degradation impact of the decisions at time t is *approximated* by employing the above linear battery degradation cost model $\alpha_{deg}|P_t^{batt}|$. This ensures that the optimization problem remains efficiently solvable. The linear cost coefficient α_{deg} is a tunable parameter.

In addition, the optimization has the following constraints,

$$S_t + \max(P_t^{batt}, 0) + P_t^{buy} = L_t + \max(-P_t^{batt}, 0) + P_t^{sell} \tag{12}$$

$$SOC_{t+1} = SOC_t + \eta_c \max(-P_t^{batt}, 0) - \frac{\max(P_t^{batt}, 0)}{\eta_d} \tag{13}$$

$$SOC_{min} \le SOC_t \le SOC_{max} \tag{14}$$

$$-P_{cap}^{ch} \le P_t^{batt} \le P_{cap}^{dis}, \tag{15}$$

where (12) ensures that energy supply equals demand; (13) captures the BESS SOC evolution; (14) ensures that the SOC remains within safe operating bounds; and (15) limits the charging and discharging rates to be feasible.

B. Economic Analysis and Internal Rate of Return

As the BESS charging/discharging decisions are continuously made via the stochastic MPC program, the resulting stream of revenue/payments is calculated and recorded. Meanwhile, the decisions' impact on battery degradation is accurately calculated based on the cycle-based and calendar-based BESS degradation model (cf. Section II-B3). In our evaluation, we perform a full-year's simulation of BESS operations. At the end of the year, we calculate a) the total revenue over the year and b) the degradation impact of this year's BESS operations. We then extrapolate these results into future years until the end of the life of BESS. Notably, the BESS degradation from prior years will impact the revenue/payments of future years due to the cumulative loss of BESS capacity from prior years' degradation. More details follow.

1) First Year's BESS Net Revenue and Degradation: As we are interested in the economic return of BESS, we compute the first year's *net* revenue of BESS as the *difference* between the revenue with optimized BESS operations and that without any BESS in the system (the baseline):

$$R_{annual} = R_{optimized} - R_{baseline}. \tag{16}$$

We also compute the BESS degradation indicator at the end of the first year based on (7), denoted by ΔD_{annual}.

2) Projected BESS Net Revenue to the End of Battery Life: Based on the first year's net revenue of BESS and the capacity degradation, we project the net revenue over the entire life of the BESS. Specifically, at the start of year y,

- We first compute the cumulative BESS degradation indicator as $\Delta D_{total} = (y-1) \cdot D_{annual}$.
- We next compute the remaining battery life, denoted by $C(y)$, based on (8).

- The BESS net revenue of year y is then estimated as $R_{annual} \cdot C(y)$.
- The BESS end-of-life is reached after year $y-1$ when $C(y)$ reaches the end-of-life threshold, e.g., 70%.

The projection of the net revenues in all the years until BESS's end-of-life provides the foundation for computing the return on investment of BESS.

3) Internal Rate of Return: Given different a) BESS specifications and b) operation strategies, the revenue streams and BESS lifetimes can vary significantly. For example, aggressive charging/discharging of BESS may boost the annual revenue but reduce its lifetime. To *fairly* compute and compare the return on investment of BESS under all possible revenue streams and lifetimes, we employ the *Internal Rate of Return* (IRR) as a universal metric [8]. Specifically, the IRR of a BESS is calculated based on the cash flow stream over the entire BESS lifetime, by solving the following equation,

$$-c_{batt} + \sum_{y=1}^{Y_{life}} \frac{R_{annual} \cdot C(y)}{(1+IRR)^y} = 0, \tag{17}$$

where c_{batt} is the initial capital cost of battery investment, $C(y)$ is the BESS remaining life at the start of year y, and Y_{life} is the total battery life time in years.

C. Simulation Environment

As discussed above, realistic simulations of the BESS operations that represent real-world situations are essential for accurately evaluating the return on investment of BESS.

1) Real-World Data Used for Simulations: We use three types of real-world data in our simulations: a) electricity prices, b) electric loads, and c) solar energy generation. In simulating BESS's decision making, however, while prices and loads are assumed to be known, *future* solar generation is not. This is despite the use of real-world solar generation data in evaluating the BESS decisions. As such, *forecast* of future solar generation in the prediction horizon of the stochastic MPC needs to be generated at every hour.

2) Solar Generation Forecast: At each hour, hourly forecasts of solar generation in the prediction horizon (e.g., the next 24 hours) are generated based on a) the real-world historical data of solar generation in this prediction horizon, and b) an Ornstein–Uhlenbeck (OU) process [12]. Specifically,

$$\epsilon_t^{(1)} = (1-\phi) \cdot \epsilon_{t-1}^{(1)} + \sigma \cdot \xi_t \tag{18}$$

$$\log(F_t) = \log(H_t) + \epsilon_t^{(1)}, \tag{19}$$

where $\epsilon_t^{(1)}$ is the residual of the OU process at time t, and $\xi_t \sim \mathcal{N}(0,1)$. ϕ and σ are the OU process parameters controlling the mean-reversion effect and the volatility of the random innovation. H is the real-world data of solar generation in the prediction horizon. F is the forecast generated. Notably, the log function is employed to ensure that the generated solar values are non-negative. In essence, $\epsilon_t^{(1)}$ represents the forecast errors (in log scale) which follow an OU process with reversion to a mean of zero. Next, upper limit S_{max} are applied to prevent physically unrealistic solar generation values:

$$\epsilon_t^{(1)} \leftarrow \min(\epsilon_t^{(1)}, \log(S_{max}) - \log(H_t)). \tag{20}$$

We note that the purpose of the above implementation is for the realistic simulation of forecasts. In real-world operations, solar energy forecasting in the prediction horizon will need to be performed (or obtained via forecasters).

3) Scenario Generation of Solar Energy: In stochastic MPC, solar generation scenarios need to be generated based on the solar generation forecast F. For this, we apply the same OU process again to create multiple realistic scenarios for the prediction horizon. Importantly, the forecast is now used as input to generate scenarios:

$$\epsilon_{s,t}^{(2)} = (1-\phi) \cdot \epsilon_{s,t-1}^{(2)} + \sigma \cdot \xi_{s,t} \tag{21}$$

$$\log(S_{s,t}) = \log(F_t) + \epsilon_{s,t}^{(2)}, \tag{22}$$

where $S_{s,t}$ represents scenario s at time t, and the noise terms $\xi_{s,t} \sim \mathcal{N}(0,1)$ are independent across scenarios. The same upper limit is applied to prevent unrealistic solar generation:

$$\epsilon_{s,t}^{(2)} \leftarrow \min(\epsilon_{s,t}^{(2)}, \log(S_{max}) - \log(F_t)). \tag{23}$$

4) Parameter Calibration: The OU process parameters ϕ and σ control the characteristics of both forecasting and scenario generation. The two parameters can be calibrated using real-world data of solar forecast and realizations of *different forecast horizons*. The initial residual (i.e., forecast error) $\epsilon_0 = 0$. The first hour forecast error is just the random innovation term, with no mean-reversion. Therefore, σ can simply be estimated from the statistics of the hour-ahead forecast errors. Next, with the real-world forecast error statistics for a different forecast horizon (e.g., 2-hour-ahead), the other parameter ϕ can then be estimated.

IV. Simulation and Evaluation

A. Simulation Setup

We utilize the data from a real-world household in Austin, Texas, whose loads and solar generation are recorded for an entire year [13]. The loads are scaled to an average of 30kWh per day to represent an average U.S. household. The electricity prices follow a TOU structure in [14], as depicted in Fig. 2. Excessive energy can be sold to the grid at a lower price, in particular, 9.91 cent/kWh according to [14]. In the default setting, the household has a 7.5kW rooftop solar PV system.

We consider installing a BESS in the household. The battery has a range of energy and power capacity to choose from, with charging and discharging efficiency $\eta_c = \eta_d = 95\%$, $SOC_{min} = 2\% E_{cap}$, and $SOC_{max} = 98\% E_{cap}$. The default cost of energy component and power inverter component are $\pi_E = \$200/kWh$ and $\pi_P = \$300/kW$. (In comparison, a Tesla Powerwall 3 with 13.5kWh energy capacity and 11.5kW power capacity costs $\$8,200$ in July 2025, not including tax credit and installation cost.) The battery can operate 6,000 full cycles before reaching the end-of-life condition at 70% capacity. We treat the linear degradation cost coefficient α_{deg} used in optimization as a hyperparameter to control the aggressiveness of battery operation, i.e., with higher α_{deg}, the battery would operate more conservatively. The default $\alpha_{deg} = 0$, because a) it is a simple choice without the need for tuning, and b) it consistently leads to near-optimal

BESS operations in our tested settings. Calendar degradation coefficient $\alpha_{calendar} = 0.02$ per year, which translates to a maximum of 50 years of shelf life with no operation. In the non-linear degradation model, $\alpha_{sei} = 5.75\text{e}{-2}$, and $\beta_{sei} = 121$ according to [9]. For the log-OU process, the two parameters are fitted with real-world solar forecast and realization data in [15], with $\phi = 0.3674$, and $\sigma = 0.4233$. A total of 10 forecast scenarios, each of length 24, are generated at each hour for MPC optimization.

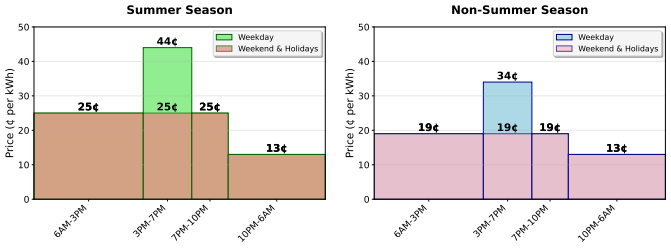

Fig. 2. TOU electricity rates for summer and non-summer seasons, showing weekday and weekend/holiday pricing across different time periods.

B. Cost-benefit Analysis for Various E_{cap} and P_{cap}

We first study what the best BESS specification is that yields the highest return on investment. Table I and II list the IRR and annual net benefit of a wide selection of BESS specifications. A heatmap visualization of Table I is shown in Fig. 3, with lighter color indicating higher IRR. First, it is evident that, the smaller the BESS's energy capacity, the higher the IRR. This is simply due to the diminishing marginal return principle (as we do not consider fixed installation cost.) We see that, for energy capacity below 7.5kWh, 4-hr duration BESS achieves the highest IRR — Notably, very high IRRs above 10% can be achieved in all these cases. From Table II, we observe that having higher power capacity (i.e., shorter duration with the same energy capacity) often leads to a higher annual net profit. This is because higher power capacity enables more aggressive charging/discharging. However, this also increases the degradation costs and hence reduces BESS's lifetime. In general, increases in both degradation and initial investment lead to lower IRRs.

TABLE I
INTERNAL RATE OF RETURNS (IRRS) FOR VARIOUS BATTERY ENERGY CAPACITY AND DURATION

E_{cap} (kWh)	1h	2h	4h	6h	8h	10h
1.25	5.6%	14.3%	16.3%	14.9%	12.5%	10.7%
2.50	5.0%	12.6%	15.2%	14.2%	12.1%	10.4%
5.00	2.7%	9.1%	12.5%	12.4%	11.0%	9.6%
7.50	0.8%	6.5%	10.0%	10.4%	9.6%	8.8%
10.00	-0.1%	4.8%	8.3%	9.0%	8.6%	8.0%
12.50	-0.4%	3.9%	7.2%	7.9%	7.8%	7.3%
15.00	-0.7%	3.2%	6.2%	7.1%	7.0%	6.7%
17.50	-0.9%	2.6%	5.3%	6.3%	6.4%	6.1%

We further depict IRR versus hour duration in Fig. 4. The green and red dashed lines in the figure mark where IRR=6% and where IRR=0, respectively. We can see that the duration of 4 to 6 hours is the sweet spot for the default setting.

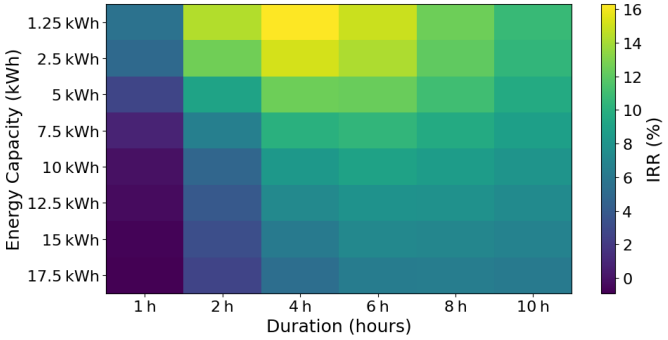

Fig. 3. Heatmap of battery IRR across energy capacities and duration ratings.

TABLE II
ANNUAL NET PROFIT OF BATTERY ($) FOR VARIOUS BATTERY SIZES

E_{cap} (kWh)	1h	2h	4h	6h	8h	10h
1.25	107.1	101.8	80.2	63.2	50.6	42.0
2.5	183.2	176.8	149.7	121.5	98.7	82.3
5	279.9	278.3	253.2	218.3	183.4	155.8
7.5	341.7	342.2	324.4	287.8	250.6	217.9
10	384.6	385.8	375.8	339.0	300.8	266.6
12.5	413.7	415.4	409.9	377.9	339.8	305.2
15	430.7	431.3	430.2	406.8	371.0	336.7
17.5	440.9	441.0	441.5	427.8	397.0	363.7

C. Sensitivity Analyses

We next perform a sensitivity analysis of various factors, including battery capital cost, linear cost coefficient, and energy selling price. We evaluate the following two battery specs: default specs with E_{cap}=7.5kWh, P_{cap}=1.8kW (4-hr duration), and the Tesla Powerwall 3 with E_{cap}=13.5kWh, P_{cap}=11.5kW.

1) IRR sensitivity to battery cost: We vary the battery capital cost coefficients according to the battery cost projection in [16], and calculate the IRR for the projected cost in 2030, 2040, and 2050. As shown in Fig. 5, we see that Powerwall 3's specs achieve a much lower IRR compared with our default specs, likely because its high energy and power capacity are *too large to be fully utilized* for consumers with the average load and solar energy sizes.

2) IRR sensitivity to linear cost coefficient: Previously, we mentioned that the linear cost coefficient used in optimization

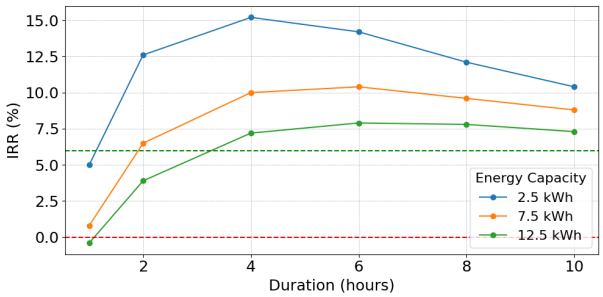

Fig. 4. Internal Rate of Return (IRR) versus duration for three battery energy capacities (2.5kWh, 7.5kWh, and 12.5kWh).

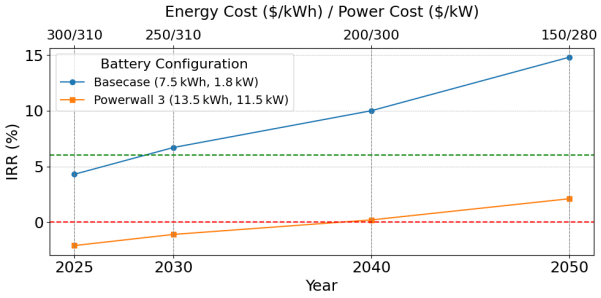

Fig. 5. IRR sensitivity to battery costs projected over time for basecase (7.5kWh/1.8kW) and Powerwall 3 (13.5kWh/11.5kW) settings.

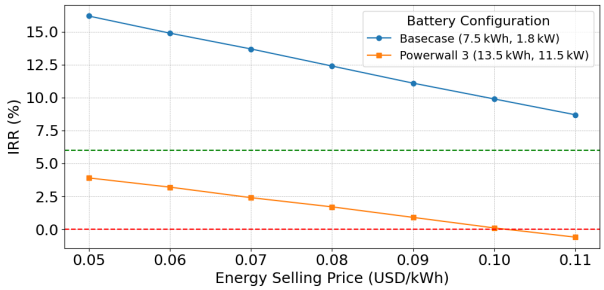

Fig. 7. IRR sensitivity to energy selling price (USD/kWh) for the default specs (7.5kWh/1.8kW) and the Powerwall 3 specs (13.5kWh/11.5kW).

is a hyperparameter that controls the operation aggressiveness of BESS. The sensitivity analysis for linear degradation cost is shown in Fig. 6. We can see that the linear degradation costs of 0.01-0.03 yield the highest IRR, by balancing profit-making and degradation. This implies that the IRRs achieved with our simple default of zero linear degradation cost, as shown in the previous tables and figures, can be made even higher if specs-specific tuning is performed for this linear cost coefficient.

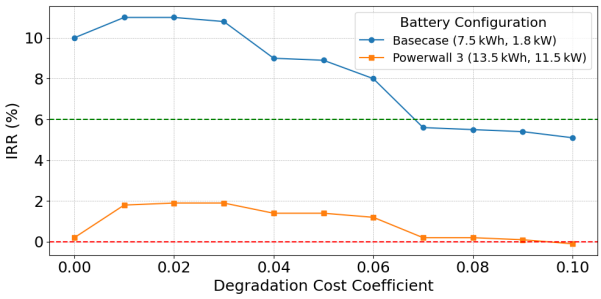

Fig. 6. IRR sensitivity to linear degradation cost coefficient for basecase (7.5kWh/1.8kW) and Powerwall 3 (13.5kWh/11.5kW) settings.

3) IRR sensitivity to energy selling price: Last but not least, we consider alternative cases where energy selling price vary between $0.05/kWh and $0.11/kWh, which are all lower than the lowest price in TOU pricing programs, so that there is no opportunity for BESS to simply arbitrage. Fig. 7 shows that, as the selling price decreases, the IRR gets higher. This is because the alternative of PV charging to battery is selling to the grid: when this alternative becomes less attractive, having a BESS would bring more net profit.

V. Conclusion

We studied the economic viability of BESS for residential consumers with rooftop solar. Hourly charging/discharging decisions are optimized using a stochastic model predictive control framework. As time progresses, solar generation scenarios over the prediction horizon are repeatedly generated based on updated forecast information. The impact of the optimized BESS charging/discharging decisions on BESS degradation is computed based on accurate degradation models. Based on the entire history of BESS charging/discharging decisions, the revenue/payments stream and degradation process are computed from which the return on investment of BESS over its entire lifetime is evaluated. Specifically, the Internal Rate of Return (IRR) is employed as the metric that fairly compares BESS with different specifications and lifetimes. Optimal BESS sizing with the highest IRR is identified accordingly.

References

[1] California Energy Commission, "2019 building energy efficiency standards - solar requirements," 2020. [Online]. Available: https://www.energy.ca.gov/programs-and-topics/programs/building-energy-efficiency-standards/2019-building-energy-efficiency

[2] California Public Utilities Commission, "Decision on net energy metering reform," 2022, decision 22-12-056. [Online]. Available: https://www.cpuc.ca.gov/industries-and-topics/electrical-energy/demand-side-management/net-energy-metering

[3] M. Chowdhury, M. Rao, Y. Zhao, T. Javidi, and A. Goldsmith, "Benefits of storage control for wind power producers in power markets," *IEEE Transactions on Sustainable Energy*, vol. 7, no. 4, pp. 1492–1505, 2016.

[4] M. B. Abdelghany, A. Al-Durra, H. Zeineldin, and F. Gao, "Integrating scenario-based stochastic-model predictive control and load forecasting for energy management of grid-connected hybrid energy storage systems," *Int. J. Hydrogen Energy*, vol. 48, no. 91, pp. 35 624–35 638, 2023.

[5] L. Santosuosso, S. Camal, F. Liberati, A. Di Giorgio, A. Michiorri, and G. Kariniotakis, "Stochastic economic model predictive control for renewable energy and ancillary services trading with storage," *Sustainable Energy, Grids and Networks*, vol. 38, p. 101373, 2024.

[6] J. Li, J. Zhou, and B. Chen, "Review of wind power scenario generation methods for optimal operation of renewable energy systems," *Applied Energy*, vol. 280, p. 115992, 2020.

[7] F. Wankmüller, P. R. Thimmapuram, K. G. Gallagher, and A. Botterud, "Impact of battery degradation on energy arbitrage revenue of grid-level energy storage," *Journal of Energy Storage*, vol. 10, pp. 56–66, 2017.

[8] S. P. Boyd and L. Vandenberghe, *Convex optimization*. Cambridge university press, 2004.

[9] B. Xu, A. Oudalov, A. Ulbig, G. Andersson, and D. S. Kirschen, "Modeling of lithium-ion battery degradation for cell life assessment," *IEEE Transactions on Smart Grid*, vol. 9, no. 2, pp. 1131–1140, 2018.

[10] Y. Shi, B. Xu, Y. Tan, D. Kirschen, and B. Zhang, "Optimal battery control under cycle aging mechanisms in pay for performance settings," *IEEE Trans. on Automatic Control*, vol. 64, no. 6, pp. 2324–2339, 2018.

[11] S. D. Downing and D. Socie, "Simple rainflow counting algorithms," *International journal of fatigue*, vol. 4, no. 1, pp. 31–40, 1982.

[12] H. Higgs and A. Worthington, "Stochastic price modeling of high volatility, mean-reverting, spike-prone commodities: The australian wholesale spot electricity market," *Energy Economics*, vol. 30, no. 6, pp. 3172–3185, 2008.

[13] C. Holcomb, "Pecan Street Inc.: A Test-bed for NILM," in *International Workshop on Non-Intrusive Load Monitoring*, 2012.

[14] Austin Energy, "Austin energy - value of solar rate," https://austinenergy.com//rates/residential-rates/value-of-solar-rate/, 2024.

[15] H. T. Pedro, D. P. Larson, and C. F. Coimbra, "A comprehensive dataset for the accelerated development and benchmarking of solar forecasting methods," *Journal of Renew. Sustain. Energy*, vol. 11, no. 3, 2019.

[16] W. Cole and A. Karmakar, "Cost projections for utility-scale battery storage: 2023 update," National Renewable Energy Laboratory (NREL), Golden, CO (United States), Tech. Rep., 06 2023. [Online]. Available: https://www.osti.gov/biblio/1984976